A histological study of a femur of *Plagiosuchus*, a Middle Triassic temnospondyl amphibian from southern Germany, using thin sections and micro-CT scanning[•]

D. Konietzko-Meier[1,2,*] & A. Schmitt[2]

1 Uniwersytet Opolski, Katedra Biosystematyki, ul. Oleska 22, 45-052 Opole, Poland

2 Steinmann Institut, Universität Bonn, Nussallee 8, 53115 Bonn, Germany

* Corresponding author. Email: dorota.majer@uni.opole.pl

Abstract

The histology of a femur of *Plagiosuchus*, a Middle Triassic temnospondyl amphibian, is described on the basis of two supplementary methods: classic thin sectioning and micro-CT scanning. In addition, the effectiveness of high-resolution micro-CT scanning for histological analysis is assessed. A classic, mid-shaft thin section of the femur was prepared, but prior to slicing two micro-CT scans were made. One of these has an image stack of a total of 1,024 images in the horizontal plane and a slice thickness of 87.8 μm, so that the entire bone could be captured, while the second was at mid-shaft region only, yet with a higher resolution of 28.3 μm and an image stack of 787 images in the horizontal plane. The classic thin section shows a very small medullary region which is surrounded by a layer of endosteal bone. The thick cortex is highly porous with numerous large, mainly longitudinal, vascular canals arranged in layers. In the deepest cortex woven bone occurs and primary osteons had locally started to form (incipient fibro-lamellar bone), which gradually passes into parallel-fibred bone and more lamellar bone close to the outer surface. Remains of a Kastschenko line were identified, enabling a reconstruction of the entire growth record. Five Lines of Arrested Growth (LAG) could be counted. The micro-CT scan enabled observations of the ontogenetic growth stages and calculation of growth rate on the basis of a single specimen. The micro-CT scan permitted a reconstruction of the ontogenetic development and the exact deposition rate per annum. Moreover, at higher resolution the micro-CT scan revealed data on micro-anatomical characters, such as porosity and skeletochronology (growth mark count). In conclusion, micro-CT scans do provide an alternative in cases where thin sectioning of the original bone is not possible.

Keywords: long-bone histology, Kastschenko line, thin sections, micro-CT scanning, Temnospondyli, Lettenkeuper

Introduction

In recent years, histology has become a powerful tool, particularly for fossils. It has been used to infer palaeobiological issues such as growth rate and pattern, minimum age of an individual and mode of life, as well as in functional interpretations, as an additional data source (e.g., Curry, 1988, 1990; Sander, 2000; Erickson, 2001; Erickson et al., 2004; De Ricqlès et al., 2003; Sander et al., 2004; Klein & Sander, 2008; Sander et al., 2011). Growth mark (skeletochronology) count is also possible for endotherms such as birds and mammals (e.g., Chinsamy et al., 1995; Starck & Chinsamy, 2002; Köhler et al., 2012). An annual growth mark usually consists of a zone, an annulus, and ends in a Line of Arrested Growth (LAG) (see Francillon-Vieillot et al., 1990). However, this sequence may vary (e.g., Castanet et al., 1993; Konietzko-Meier & Klein, 2013). Typically, growth marks are examined in thin sections of the mid-shaft portion of long bones, preferably femora and humeri. However, this procedure is destructive to the bone and thus, in consideration of the limited amount of material, is not always possible.

The value of micro-CT scan for histological studies

Currently, it is possible to study growth marks not only in traditional thin sections but also with the help of micro-CT scans. The latter method is advantageous, because it does not cause damage to the bones. This non-destructive approach allows to 'see through' the bone and rock matrix without having to cut these. Depending on the density of bone or of the sediment, internal structures can thus be visualised. Therefore, micro-CT scanning is an effective 3D-imaging tool, which is capable of mapping morphological features and transfer them into an X-Y-Z coordinate system. Bony material can either be hidden, or displayed as a shaded shape or even in a semi-transparent guise. Snapshots of the object can hence be taken from any given angle. As early as 1990, micro-computed tomography was employed to study trabecular bone structure (Kuhn et al., 1990). Such an assessment of the diagnostic value of micro-CT scans vs the more traditional (and destructive) histological approach, however, was carried out mainly in human medicine. Holdsworth & Thornton (2002) pointed out the potential of micro-CT to quantify the density and architecture of bone. They foresaw a replacement of serial histology by micro-CT in vascular studies and in the characterisation of the phenotype of transgenic and knockout animal models during preclinical investigations.

Micro-CT scans have frequently been used in palaeontology in order to analyse and visualise bone and teeth morphology (e.g., Ponce de León & Zollikofer, 1999; Sellers et al., 2009; Ruf et al., 2010; Schwarz et al., 2010; Kin et al., 2012; Molnar et al., 2012), as well as to determine degrees of mineralisation in fossil skeletons (Sanchez et al., 2010a). On the inner architectural level of the bone, the radiological imaging was used to test bone microanatomy and to distinguish between compact and spongy portions of bone (see e.g., Hayashi et al., 2005; Moreno et al., 2007; Arbour, 2009; Houssaye et al., 2011).

Characters of the Plagiosauridae

The family Plagiosauridae Abel, 1919 is a highly characteristic group of Triassic temnospondyl amphibians. The most recent and complete review of the family, with regard to both taxonomy and geographic distribution, is that by Hellrung (2003). Two subfamilies are currently recognised, the Plagiosaurinae (which includes *Plagiosaurus* Jaekel, 1913 from the Upper Triassic of Germany and *Gerrothorax* Nilsson, 1934 from the Middle-Upper Triassic of Germany, southern Sweden and Greenland) and the Plagiosuchinae Hellrung, 2003 (which includes *Plagiosuchus* Von Huene, 1922 from the Middle Triassic of Germany and *Plagioscutum* Shishkin, 1986 from coeval strata in Russia). Furthermore, plagiosaurid remains have been recorded from the Lower Triassic of Australia (Warren, 1995), the Upper Triassic of Thailand (Suteethron et al., 1988) and the Upper Triassic of Poland (Dzik et al., 2008). However, current data on plagiosaurid anatomy are poor. The best known representatives are species of *Gerrothorax*, of which cranial and post-cranial remains, including articulated skeletons, are known (Fraas, 1913; Nilsson, 1934, 1937, 1946; Jenkins et al., 1994; Hellrung, 2003). Other specimens are exclusively known from scant cranial and post-cranial material (Fraas, 1889, 1913; Jaekel, 1913; Von Huene, 1922; Konzhukova, 1955; Shishkin, 1967, 1986, 1987; Suteethorn et al., 1988; Novikov & Shishkin, 1992; Warren, 1995; Dzik et al., 2008; Damiani et al., 2009).

The anatomical data allow to portray plagiosaurids as dorsoventrally flattened animals, completely covered by dermal armour. They are of medium size, with a total body length of usually less than one metre. Plagiosaurids are characterised by a highly modified skeleton adapted to an exclusively aquatic, bottom-dwelling mode of life (Nilsson, 1946; DeFauw, 1989; Hellrung, 2003; Damiani et al., 2009). The skull is short but wide, with enlarged orbits and prominent dermal sensory grooves. Massively built dermal pectoral girdles and robust, fully cylindrical vertebral centres with intervertebral neural arches are typical of the post-cranial skeleton. Beyond this very general 'Bauplan' of plagiosaurids, the adequately known members of the group display remarkably divergent, highly autapomorphic cranial morphologies which are used for taxonomic assessment and interpretation of their modes of life (Hellrung, 2003; Damiani et al., 2009; Schoch & Witzmann, 2012).

Previous studies of plagiosaurid histology

The histology of plagiosaurids is poorly known. De Ricqlès & De Buffrénil (2001) mentioned the pachyostosic condition in a rib of *Gerrothorax*, while Sanchez et al. (2010b, fig. 3F, G) described the histology of femora of two species of *Gerrothorax* (*Gerrothorax* sp. 1 (Staatliches Museum für Naturkunde Stuttgart, SMNS 81460) and *Gerrothorax* sp. 2 (SMNS 81475)). Both bones have been considered to have belonged to adult individuals on the basis of skeletochronological data (Sanchez et al., 2010b). The cross-section of the smaller specimen, SMNS 81460, is pyriform, similar to juvenile *Dutuitosaurus* and *Metoposaurus* (Steyer et al., 2004; Konietzko-Meier & Klein, 2013). In the other specimen, SMNS 81475, the pyriform shape is disturbed by the convex dorsal surface. The histological framework also differs in both sections. The femoral section of *Gerrothorax* sp. 1 shows pachyosteosclerotic features with an extended region of cortex and a small medullary region, which is infilled by endochondral bone and contains remains of calcified cartilage (Sanchez et al., 2010b). The innermost single thick layer of highly vascularised bone is followed by a thin external layer of avascular bone containing three or four LAGs (Sanchez et al., 2010b). *Gerrothorax* sp. 2 reveals osteoporotic features with large bays of erosion originating from the vascular canals and blurring the boundary of the medullary cavity. The inner cortex contains three well-preserved annuli; the remains of two additional annuli are

visible, which alternate with well-vascularised zones. The external cortex consists of a thick avascular layer containing two LAGs (Sanchez et al., 2010b, fig. 3F).

Witzmann & Soler-Gijón (2010) described the histology of plagiosaurid osteoderms. In *Plagiosuchus*, the entire trunk was not covered with plate-like osteoderms as in *Gerrothorax*, but with a single row of osteoderms situated on top of the neural spines. The *Plagiosuchus* osteoderms did not show the typical diploë structure which normally consists of a thick, trabecular middle region, framed by thin, compact inner and external cortices (Witzmann, 2009). Plagiosuchus osteoderms are very massive, with a thick and compact middle layer and poorly vascularised external and internal regions, and might be interpreted to have served for buoyancy reduction and stabilisation of the trunk in these aquatic animals (Witzmann & Soler-Gijón, 2010).

Aims

The main objective of the present study is to document the histology of a femur of *Plagiosuchus* for the first time, on the basis of two independent sources: the classic thin section and micro-CT scanning, as an additional tool for the study of the life history coded in the histological framework of long bones.

Material and methods

Material and locality

For the present study, a left femur (78 mm in length) of *Plagiosuchus* sp. (Muschelkalkmuseum Hagdorn, Ingelfingen; MHI 1078/16) from the so-called 'Lettenkeuper' (Middle Triassic) of Wolpertshausen-Heidehöfe (Germany) has been studied. This particular specimen was collected in 1978 during the construction of motorway A6. It originates from Bed 11 of the 'Untere Graue Mergel' (Geyer et al., 2005). This unit constitutes the siliciclastic-carbonate member of the upper Erfurt Formation (Lower Keuper) and is of Ladinian age (Geyer et al., 2005). Bed 11 has a thickness of 12 to 17 centimetres. Apart from invertebrate remains, the locality has also yielded well-preserved vertebrates such as numerous amphibians (*Mastodonsaurus*, *Kupferzellia*, *Plagiosuchus* and *Gerrothorax*). Rauisuchians such as *Batrachotomus* are less common. Additionally, cynodonts and numerous isolated scales of the actinopterygian fish *Serrolepis* have been found (Hagdorn, 1980).

Methods

Thin sections

The femur was cross-sectioned at mid-shaft length (Fig. 1A) according to standard petrographic procedures (Stein & Sander, 2009). The thin section was then ground and polished to a thickness of about 60-80 µm using wet SiC grinding powders (SiC 600, 800). Subsequently, it was studied under a LEICA DMLP light microscope in normal and polarised light. Cross-sections were scanned with an Epson V740 PRO high-resolution scanner.

Micro-CT scan

Prior to cross-sectioning, the femur was prepared free from the matrix, after which it was micro-CT scanned with a v|tome|x s by GE phoenix|x-ray at the Steinmann Institute of Geology, Mineralogy and Palaeontology (University of Bonn). With this equipment, data are generated using an X-ray tube as a source
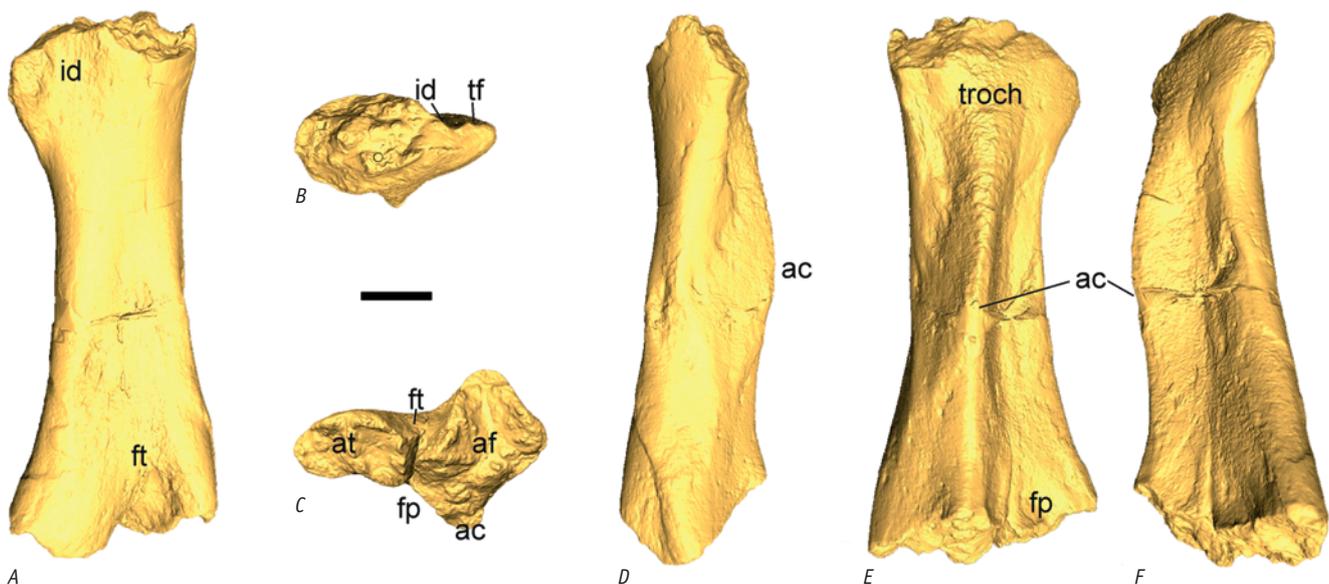

Fig. 1. *Morphology of the* Plagiosuchus *femur (MHI 1078/16), as reconstructed from the micro-CT scan in dorsal (A), proximal (B), distal (C), posterior (D), ventral (E) and anterior (F) views. Abbreviations: ac – adductor crest; af – surface for fibula; at – surface for tibia; ft – fossa tendinalis; fp – fossa poplitea; id – iliac depression; tf – trochanteric flange; troch, trochanter. Scale bar equals 10 mm.*

that irradiates an object on a rotating table in front of a detection surface. Depending on the setting, the angular movement from one rotation step to the next can be as high as one-fifth of a degree. Depending on the size of the object the resolution may vary, as it depends on how close the X-ray tube is to the object. The resolution determines the slice thickness of the above-mentioned images. Hence, the micro-CT produces a volume of data that can be worked out in order to demonstrate various structures of different density, as a change in density alters the ability of a structure to block the X-ray beam.

For the present study two scans of the femur were made. The first comprises the entire bone and contains 1,024 images in the horizontal plane at a slice thickness of 87.8 µm. The second scan covered the horizontal plane of the mid-shaft region at a higher resolution of 28.3 µm and 787 images. The higher resolution scan was produced in order to detect more histological details, whereas the lower resolution scan (87.8 µm) was used to reconstruct the outer surface of the entire bone and to visualise its growth cycles (see Fig. 5). In order to compare the classic thin section with the micro-CT image, one image from approximately the same plane was chosen out of the high-resolution scan image stack (28.3 µm).

The images are generated in the vertical plane only. 3D software allows this volume of data to be reformatted in various planes afterwards. In this case, the data were processed and bundled into image stacks with the help of VGStudio MAX 2.0 software from Volume Graphics GmbH. Later the data were transformed into a volumetric representation of the structure.

The virtual images were processed on a 64-bit PC workstation with 8 GB of RAM, running on Microsoft Windows® 7 Professional. Zones have a lower density and appear dark in the images. They were digitally highlighted with AVIZO® 6.3 and AVIZO® 7.0 and were marked with a green colour (Fig. 4C).

Terminology

Histological terminology follows Francillon-Vieillot et al. (1990). In the present sample, zones and LAGs appear regularly, but the annuli do not. Thus, the succession of one zone and one LAG is considered to be indicative of a completed annual growth cycle in *Plagiosuchus*.

Results

Morphology of femur

The shaft of MHI 1078/1 (Fig. 1) is straight, dorsally flat and ventrally convex. The convexity results from the very prominent adductor crest, which rises from the distal end, from the posterior articulatory surface (with the fibula) in proximal direction. Near the proximal head it merges into the trochanter, which is situated in the centre on the ventral side (Fig. 1C, E). On the dorsal side the axial symmetry is emphasised by the long *fossa tendinalis*, which starts at mid-length (Fig. 1A, C). In proximal view, the head is flat with a small trochanteric flange on the anterior side. The proximal articular surface is concave on the dorsal side with a distinct iliac depression and flat on the ventral side (Fig. 1B); however, the proximal head is slightly damaged and cannot be described in detail. On the distal end, the articulation surfaces for the tibia and fibula are well developed. The surface for the fibula is considerably larger and rectangular in distal view, while that for the tibia is flatter and almost perpendicular to the previous (Fig. 1C). Between both surfaces the prominent fossa tendinalis is visible on the dorsal side and a flatter *fossa poplitea* on the ventral side (Fig. 1C).

Histological description based on thin sections

As a result of the prominent adductor crest, the mid-shaft cross-section is triangular (Fig. 2A).The boundary between the endochondral and periosteal domains cannot be determined because of the breakage of the secondary trabeculae system within the medullary region.

The entire primary cortex is highly vascularised. On the dorsal side the vascular canals are organised in regular rows of mostly longitudinal, occasionally reticular, vascular canals (Fig. 2A). In the adductor crest region, vascular canals are considerably larger and are directed radially. In some areas of the inner cortex vascular canals started to develop into primary osteons, others show signs of resorption and secondary deposition of lamellar bone. In the external part of cortex mostly simple vascular canals are present.

The primary cortex consists largely of parallel-fibred bone (Fig. 2E, F), which alters gradually near the anterior margin into lamellar bone (Fig. 2G, H). In the deep part of cortex woven bone occurs and primary osteons started to form constituting incipient fibrolamellar bone (Klein, 2010; Konietzko-Meier & Klein, 2013; see Fig. 2C, D).

Five LAGs can be identified all around the cross-section as distinctly darker lines (Fig. 2A), except at the top of the adductor crest area where no LAGs are visible.

In the entire section Sharpey's fibres are deposited (Fig. 2B); these constitute an extremely dense net in the adductor crest region and at the postero-dorsal region, where there is a concentration of thick, perpendicular fibres which are oblique to the bone surface.

The border between cortex and medullary region is difficult to determine, on account of the destruction of the inner part of the section. However, between the broken trabeculae in the central part of section, short layers of periosteal and endosteal bone with calcified cartilage in between are visible in a few places (Fig. 3A, B), which may help to reconstruct the area of the medullary region (for details see below).
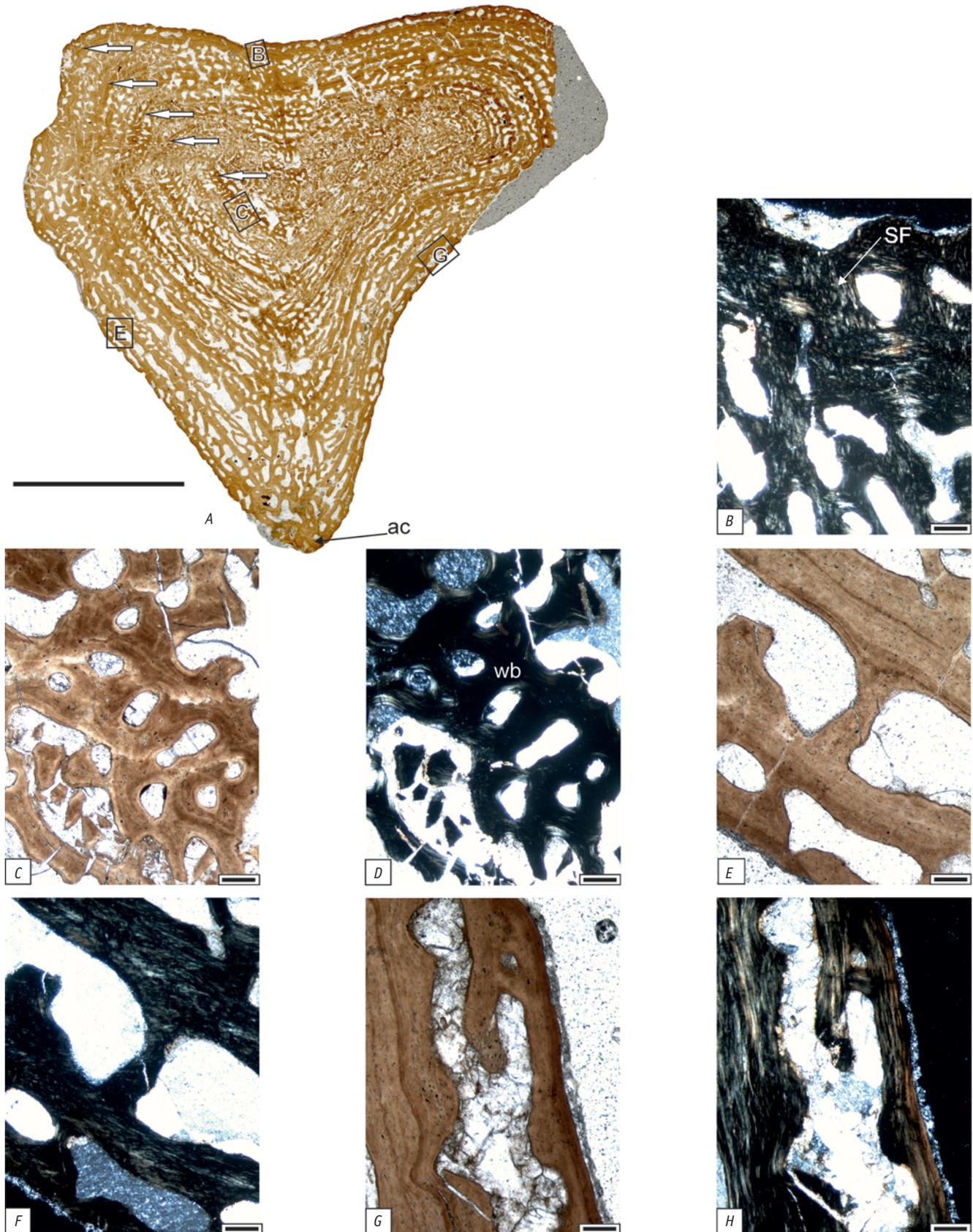
Fig. 2. *The general histology of the* Plagiosuchus *femur (MHI 1078/16); A. Microstructure at mid-shaft in cross-section; white arrows refer to LAGs (ac = adductor crest); B. Close-up of dorsal part of cortex with Sharpey's fibres (= SF), in polarised light; C. Deep part of cortex in normal light; D. the same view as in C, with woven bone (= wb), in polarised light; E. The cortex exhibiting parallel-fibred bone in normal light; F. The same view as in E, but in polarised light; G. Lamellar bone visible in anterior area of external part of the cortex; H. The same view as in G, in polarised light. Scale bars equal 10 mm (A) and 100 μm (B-H).*

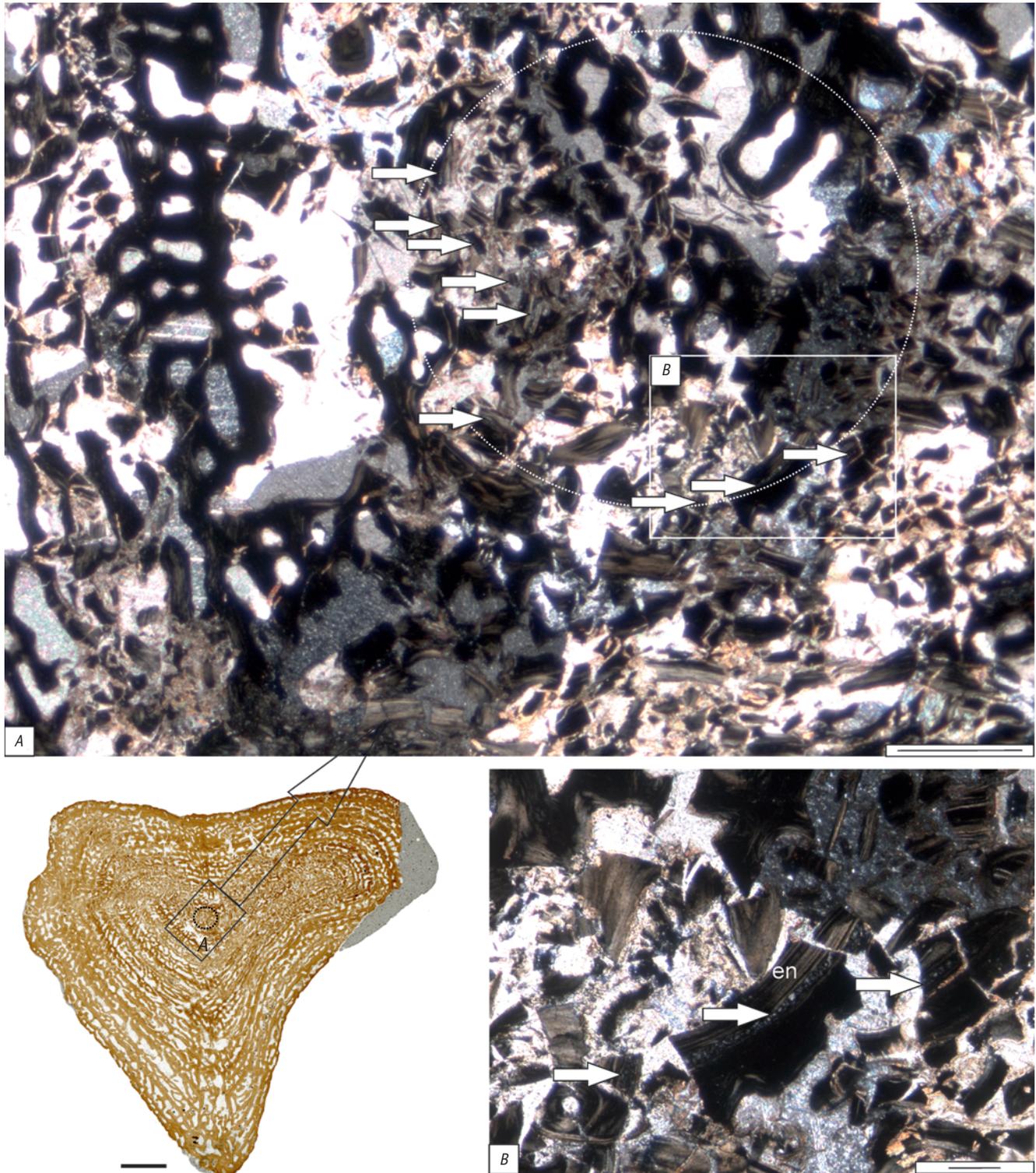Fig. 3. The medullary region of the Plagiosuchus femur (MHI 1078/16); A. medullary region in polarised light; the white arrows denote remains of calcified cartilage. The dashed line shows the probable area of medullary region. The photomicrograph below shows the area of enlargement visible in A; B. close-up of medullary region with visible remains of the Kastschenko line (white arrows) and endosteal bone (= en). Scale bar equals 10 mm (cross-section), 500 μm (A) and 100 μm (B).

Micro-CT scan images

In the high-resolution micro-CT scan, the inner bone structure can be distinguished as a sequence of variable grey-scale layers (Fig. 4A, B). The comparison between the classic thin section and high-resolution micro-CT image from the same plane allows interpretation of the different colours. The largest vascular canals are black; tissue of lower density, i.e. bone with numerous,
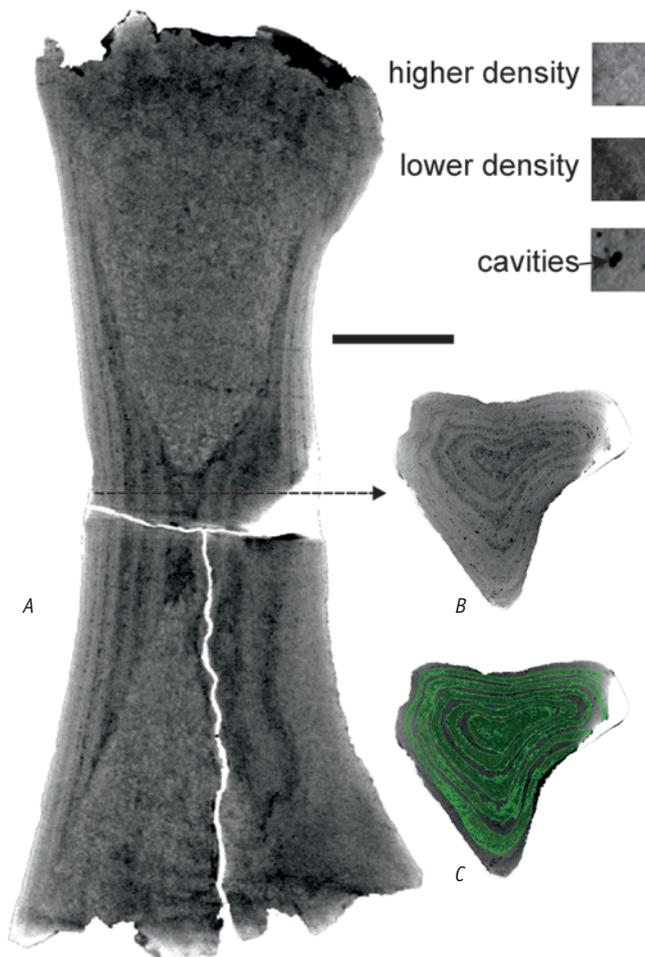
Fig. 4. *Micro-CT scan images of the* Plagiosuchus *femur (MHI 1078/16) in longitudinal view with 1,024 images in the horizontal plane at a slice thickness of 87.8 µm (A) and cross-section with a higher resolution of 28.3 µm and 787 images in the image stack (B). Visualisation of the area of zones (C). The green colour marks the area of zones visible in cross-section; the black arrow denotes the plane of sectioning. Scale bar equals 10 mm.*

smaller canals is dark grey, and that of higher density (i.e., higher organisation; the permanent layer of highly mineralised bone) appears as light grey or white (Fig. 4). In MHI 1078/16, a concentration of linear, large vascular canals is visible as dark circular layers; grey layers correspond to rows of smaller canals and larger amounts of bone tissue in between, and finally the LAGs, which are very intensely mineralised, appear as light grey or white lines (Fig. 4B).

The same sequence of alternating dark- and light-coloured layers is visible in the scan of lower resolution (Fig. 4A). In the longitudinal planes, especially on the posterior side of the bone, light and dark grey layers can be distinguished. The lighter lines represent the higher mineralised tissue (LAGs), and thus each dark layer together with a light line correspond to a single annual growth cycle. Altogether, as in the thin section, five annual growth cycles can be traced in the micro-CT scan (Fig. 5A, B).

The annual growth cycles visible in the low-resolution scan allow a relatively detailed picture of successive growth stages of the entire bone (Fig. 6C). The probably cartilaginous precursor of bone is visible in the longitudinal as a dark spot in the middle of the section; it is merely ca 12 mm long and the diameter at mid-shaft in the posterior-anterior direction is ca 2 mm (Fig. 6A). The final bone measures 78 mm in length and is almost 20 mm in perimeter (Fig. 6A). The average growth in length per annum is regular, around 10 mm. The rate of increase of the mid-shaft perimeter shows a different tendency. The cortex thickness is closely related to morphology; deposition of the bone was slower on the posterior side (Figs 1A, 6A), whereas it was more rapid anteriorly. The highest increase in cortex thickness appears in the adductor crest region. However, appositional growth per cycle/year in mm seems to have been relatively proportional throughout life with a slight tendency for a decrease in growth rate between the last two points (Fig. 6B).
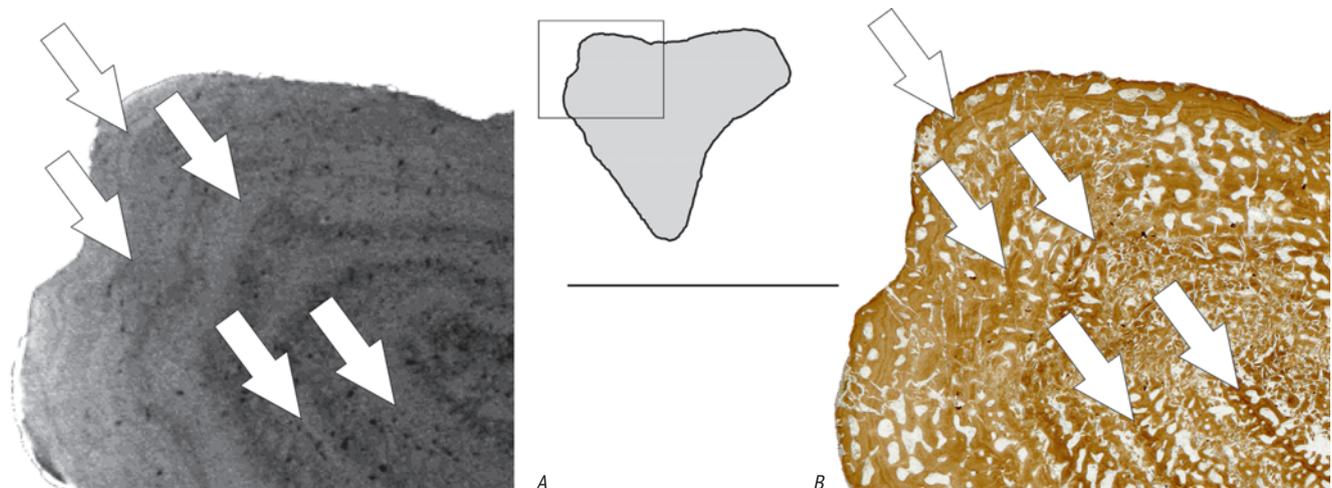

Fig. 5. *Comparison between micro-CT image (A) with a resolution of 28.3 µm and 787 images and classic thin section (B) from mid-shaft of the* Plagiosuchus *femur (MHI 1078/16). Note that five LAGs (white arrows) are visible in both. Scale bar equals 10 mm.*
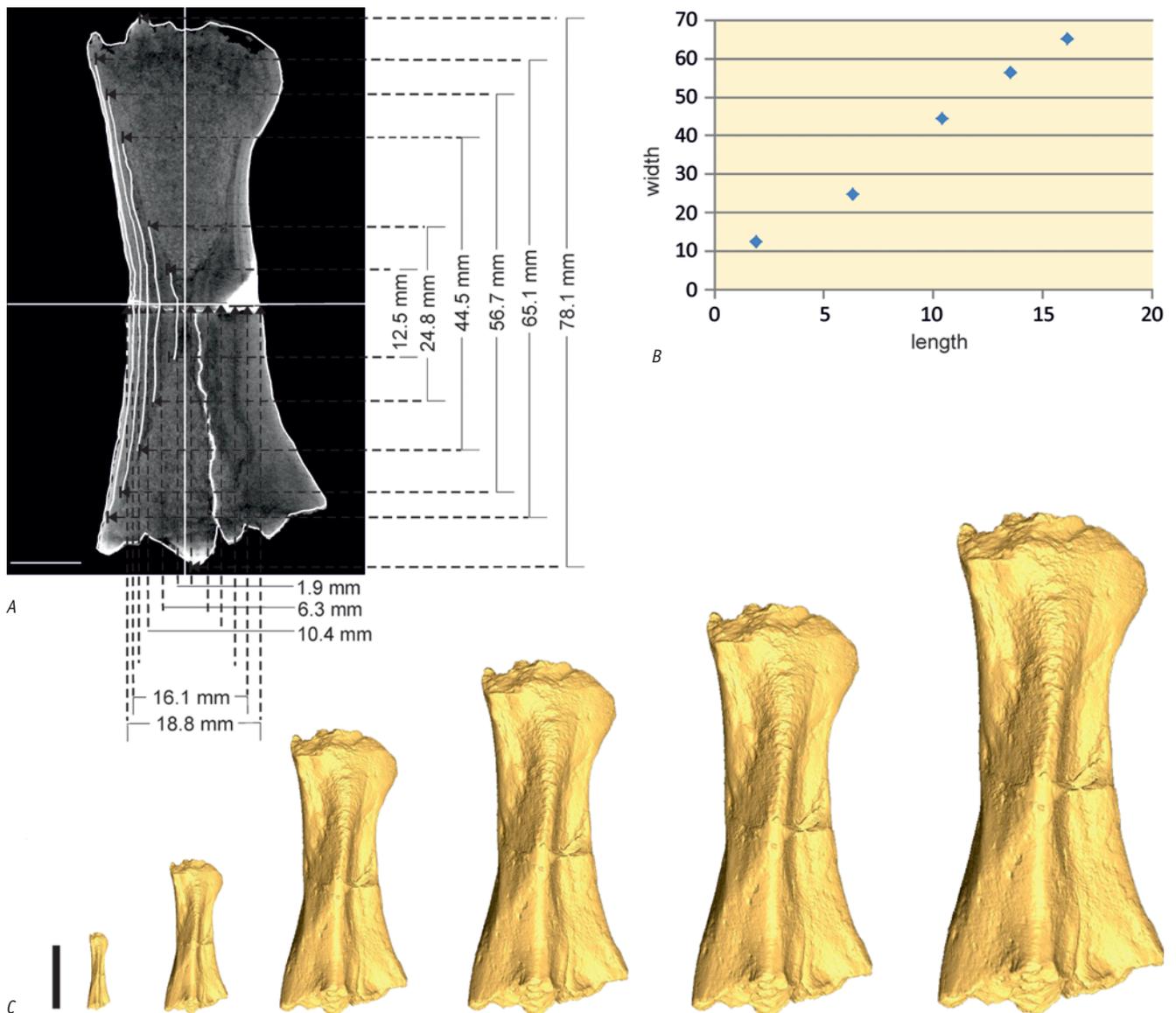
Fig. 6. Reconstruction of growth dynamics of the Plagiosuchus *femur (MHI 1078/16); A. measurement of virtual ontogenetic series on the basis of micro-CT scan image (resolution: 1,024 images in the horizontal plane at slice thickness of 87.8 μm); B. graph showing the proportion between length of the entire bone and width at mid-shaft in successive stages; C. reconstruction of bone size during growth. Note that for easier imaging of successive bones from virtual ontogenetic series the same reconstruction but with changed proportions was used. Scale bars equal 10 mm.*

Discussion

Reconstruction of the medullary region

Remains of calcified cartilage that are visible in the central part of the section (Fig. 3) have a highly characteristic structure. The cartilage is lined by a thin layer of periosteal bone on the outer surface and a thin layer of endosteal on its inner surface (Fig. 3B). This structure resembles the Kastschenko line (KL). As suggested by Castanet & Smirina (1990), a thin layer of cartilage situated between the periosteal and endosteal bone probably is the remnant of the larval cartilage precursor. Originally described as 'Wandstandiger Knorpel' by Kastschenko (1881), it has been identified to define accurately the endosteal

resorption in amphibians (Haines, 1942; Rozenblut & Ogielska, 2005). The Kastschenko line indicates that the innermost periosteal bone had not yet fully resorbed (Francillon-Vieillot et al., 1990) and, thus, that the growth record is complete.

On the basis of the position of the KL, a reconstruction of the original area of the medullary region is possible (Fig. 3). The medullary region was very small compared to the thickness of the cortex; in the dorsal-ventral axis the medullary region comprises approximately 6% of the whole section only (Fig. 3A). However, it is difficult to determine if the pieces of the trabecular system visible in the central part of the section have a periosteal or endochondral origin and to draw conclusions about the character of the medullary region; either open or infilled with endochondral bone.

Growth strategies

The extremely highly vascularised cortex and the presence of incipient fibrolamellar bone in the femur MHI 1078/1 indicate that the growth rate was high in this animal. The reconstruction based on the micro-CT scan shows a very small cross-section in comparison to its final size. The length of the bone doubled during the first year of life (Fig. 6). The micro-CT scan reconstruction confirms the hypothesis of Konietzko-Meier & Klein (2013) that histological and morphological mid-shaft are not necessarily the same. The histological mid-shaft contains the earliest bone deposited, meaning that the preserved growth record is complete. The morphological mid-shaft it is the mathematical half of the actual, 'straight' shaft region without any significant morphological characters. The extremely small size of the ontogenetically earliest bone and rapid growth of *Plagiosuchus* makes identification of the histological mid-shaft very difficult. Even a small displacement of the sampling location can result in a very variable framework of medullary regions (Konietzko-Meier & Klein, 2013).

The presence of a Kastschenko line indicates that the complete growth record has been captured. The thick cortex with five LAGs, situated in relatively regular distances from each other, alternating with zones of regular rows of vascular canals suggest that the present individual probably died in its sixth year of life, at a time when its growth rate had still not decreased distinctly (Fig. 5). Additionally, there is no indication of an external concentration of LAGs.

An allometric increase in femoral size is observed (Fig. 6B). Such a remarkably stable ontogeny was also noted for *Gerrothorax pulcherrimus* (Fraas, 1913), on the basis of skull analysis (Schoch & Witzmann, 2012), with the smallest known specimens closely resembling the adults in most features. This differs markedly from the condition of dermal bone in all of the better-known Permian temnospondyls (Boy, 1988, 1990; Schoch, 2003; Witzmann, 2005, 2006; Witzmann & Schoch, 2006; Witzmann et al., 2009).

Mode of life

Various modes of life for plagiosaurids have been postulated on the basis of their skull morphology (Hellrung, 2003; Damiani et al., 2009; Jenkins et al., 2009; Schoch & Witzmann, 2012). The different histological frameworks of long bones appear to corroborate such a conclusion. Based on comparisons with extant aquatic tetrapods (De Ricqlès & De Buffrénil, 2001), Sanchez et al. (2010b) explained the differences between specimens of *Gerrothorax* as adaptation to different positions occupied in the water column. *Gerrothorax* sp. 1, which exhibits skeletal pachyosteosclerosis is heavier, possibly having favoured a bottom-dwelling life style, whereas the intense erosion process resulting in osteoporosis in *Gerrothorax* sp. 2 provided a lesser skeletal weight and thus might indicate mid-water locomotion.

Schoch & Witzmann (2012) pointed out that *Gerrothorax* was fully aquatic, but was adaptable with respect to size and nature of water body occupied.

The osteoporosis visible in MHI 1078/1 is similar to that observed in *Gerrothorax* sp. 2. However, *Plagiosuchus* with its larger body size, massive osteoderms and an extremely thick cortex, all of which added to the bone mass, seems to have been well adapted to a bottom-dwelling aquatic mode of life.

The histology of Plagiosuchus, mainly the high porosity of the primary cortex, is closely similar to that described for placodonts (De Buffrénil & Mazin, 1992; De Ricqlès & De Buffrénil, 2001; Klein, 2010) and seems to represent a similar adaptation to the aquatic environment. In interpreting life styles of plagiosaurids it is important to consider the osteodermal cover of the body. Plagiosaurids with a dense cover of numerous osteoderms on belly, flanks, gill region and neck and a large dermal pectoral girdle (interclavicle, clavicles) may reflect adaptations to aquatic environments similar to turtles or placodonts for buoyancy (Witzmann & Soler-Gijón, 2010; Witzmann, 2011). In armoured animals body density may have been evolutionarily adjusted through changes in carapace (Canoville & Laurin, 2010), or through pachyostotic ribs and a row of bony knobs along the backbone, like in placodonts.

Conclusions

Classic thin sections and micro-CT images offer a different range of opportunities in interpretation of structures. In the former, it is possible to classify the type of tissue on the basis of the orientation of collagen fibres, the degree of vascularisation and details of growth and remodelling process. The micro-CT scans do not allow analyses of tissue character, but do enable observations on the inner microanatomy from different angles along the entire bone, without loss of information; this is impossible in classic sectioning. In the current study, the micro-CT scan images clearly show that the skeletochronological data are identifiable, comparable to the classic section; however, for a correct interpretation of the X-ray images, a comparison with classic thin sections is called for. After translation of colour which is visible in the micro-CT images, further observations are possible. The micro-CT scan enables observations of growth stages and a calculation of growth rate on the basis of a single specimen. In the specimen studied here, five LAGs can be traced, and the appositional growth per cycle/year in mm could be determined on the basis of the arrangement of zones and LAGs. In conclusion, micro-CT scans provide an alternative in cases where it is not possible to thin section the original bone. Micro-CT scans yield data on growth mark count and porosity/microanatomy, but cannot replace a thin section for the study of histological details such as bone tissue. Micro-CT scanning appears to be a good supplementary method to classic thin sectioning with available skeletochronological data, although it cannot furnish a detailed analysis of tissue character.

Acknowledgements

References

Abel, O., 1919. Die Stämme der Wirbeltiere. De Gruyter (Berlin), 914 pp.

Arbour, V.M., 2009. Estimating impact forces of tail club strikes by ankylosaurid dinosaurs. PLoS ONE 4(8): e6738.

Boy, J.A., 1988. Über einige Vertreter der Eryopoidea (Amphibia: Temnospondyli) aus dem europäischen Rotliegend (?höchstes Karbon-Perm). 1. *Sclerocephalus*. Paläontologische Zeitschrift 62: 107-132.

Boy, J.A., 1990. Über einige Vertreter der Eryopoidea (Amphibia: Temnospondyli) aus dem europäischen Rotliegend (?höchstes Karbon-Perm). 3. *Onchiodon*. Paläontologische Zeitschrift 64: 287-312.

Canoville, A. & Laurin, M., 2010. Evolution of humeral microanatomy and lifestyle in amniotes, and some comments on palaeobiological inferences. Biological Journal of the Linnean Society 100: 384-406.

Castanet, J. & Smirina, E., 1990. Introduction to the skeletochronological method in amphibians and reptiles. Annales des Sciences naturelles, Zoologie (13)11: 191-196.

Castanet, J., Francillon-Vieillot, H., Meunier, F.J. & De Ricqlès, A., 1993. Bone and individual aging. *In:* Hall, B.K. (ed.): Bone. Volume 7: Bone Growth–B. CRC Press (Boca Raton): 245-283.

Chinsamy, A., Chiappe, L.M. & Dodson, P., 1995. Mesozoic avian bone micro-structure: physiological implications. Paleobiology 21: 561-574.

Curry, K., 1988. Histological quantification of growth rates in *Apatosaurus*. Abstracts of Papers, 58th Annual Meeting of the Society of Vertebrate Paleontology: 36A.

Curry, K.A., 1990. Ontogenetic histology of *Apatosaurus* (Dinosauria: Sauropoda): new insights on growth rates and longevity. Journal of Vertebrate Paleontology 19: 654-665.

Damiani, R., Schoch, R.R., Hellrung, H., Werneburg, R. & Gastou, S., 2009. The plagiosaurid temnospondyl *Plagiosuchus pustuliferus* (Amphibia: Temnospondyli) from the Middle Triassic of Germany: anatomy and functional morphology of the skull. Zoological Journal of the Linnean Society 155: 348-373.

De Buffrénil, V. & Mazin, J.-M., 1992. Contribution de l'histologie osseuse à l'interpretation paléobiologique du genre *Placodus* Agassiz, 1833 (Reptilia, Placodontia). Revue de Paléobiologie 11: 397-407.

De Ricqlès, A. & De Buffrénil, V., 2001. Bone histology, heterochronies and the return of tetrapods to life in water; where are we? *In:* Mazin, J.M. & De Buffrénil, V. (eds): Secondary adaptation of tetrapods to life in water. F. Pfeil (München): 289-306.

De Ricqlès, A., Padian, K., Horner, J.R., Lamm, E.T. & Myhrvold, N., 2003. Osteohistology of *Confuciusornis sanctus* (Theropoda: Aves). Journal of Vertebrate Paleontology 23: 373-386.

DeFauw, S.L., 1989. Temnospondyl amphibians: a new perspective on the last phases in the evolution of the Labyrinthodontia. Michigan Academician 21: 7-22.

Dzik, J., Sulej, T. & Niedźwiedzki, G., 2008. A dicynodont-theropod association in the latest Triassic of Poland. Acta Palaeontologica Polonica 53: 733-738.

Erickson, G.M., 2001. The bite of *Allosaurus*. Nature 409: 987-988.

Erickson, G.M., Makovicky, P.J., Currie, P.J., Norell, M.A., Yerby, S.A. & Brochu, C.A., 2004. Gigantism and comparative life-history parameters of tyrannosaurid dinosaurs. Nature 430: 772-775.

Fraas, E., 1889. Die Labyrinthodonten der schwäbischen Trias. Palaeontographica 36: 1-158.

Fraas, E., 1913. Neue Labyrinthodonten aus der Schwäbischen Trias. Palaeonto-graphica 60: 275-294.

Francillon-Vieillot, H., De Buffrénil, V., Castanet, J., Géraudie, J., Meunier, F.J., Sire, J.Y., Zylberberg, L. & De Ricqlès, A., 1990. Microstructure and mineralization of vertebrate skeletal tissues. *In:* Carter, J.G. (ed.): Skeletal biomineralization: patterns, processes and evolutionary trends, Vol. I. Van Nostrand Reinhold (New York): 471-530.

Geyer, G., Hautmann, M., Hagdorn, H., Ockert, W. & Streng, M., 2005. Well-preserved mollusks from the Lower Keuper (Ladinian) of Hohenlohe (southwest Germany). Paläontologische Zeitschrift 79: 429-460.

Hagdorn, H., 1980. Saurierreste ans dem Lettenkeuper im Landkreis Schwäbisch Hall. Der Haalquel 132(6): 21-23.

Haines, R.W., 1942. The evolution of epiphysis and of endochondral bone. Biological Reviews 17: 267-291.

Hayashi, S., Takemura, T., Endo, K. & Manabe, M., 2005. Utility of the X-ray CT system on bone fossils; an example of *Stegosaurus* osteoderms. Chishitsu News 6 (610): 45-49.

Hellrung, H., 2003. *Gerrothorax pustuloglomeratus,* ein Temnospondyle (Amphibia) mit knöcherner Branchialkammer aus dem Unteren Keuper von Kupferzell (Süddeutschland). Stuttgarter Beiträge zur Naturkunde B39: 1-130.

Holdsworth, D.W. & Thornton, M.M., 2002. Micro-CT in small animal and specimen imaging. Trends in Biotechnology 2002: 20 (8 Suppl.): S34-S39.

Houssaye, A., Xu, F., Helfen, L., De Buffrénil, V., Baumbach, T. & Tafforeau, P., 2011. Three-dimensional pelvis and limb anatomy of the Cenomanian hind-limbed snake *Eupodophis descouensi* (Squamata, Ophidia) revealed by synchrotron-radiation computed laminography. Journal of Vertebrate Paleontology 31: 1-6.

Jaekel, O., 1913. Über die Wirbeltierfunde in der oberen Trias von Halberstadt. Paläontologische Zeitschrift 1: 155-215.

Jenkins, F.A. Jr, Shubin, N.H. & Amaral, W.W., 1994. Late Triassic continental vertebrates and depositional environments of the Fleming Fjord Formation, Jameson Land, East Greenland. Meddelelser om Grønland, Geoscience 32: 1-25.

Jenkins, F.A. Jr, Shubin, N.H., Gatesy, S.M. & Warren, A., 2009. *Gerrothorax pulcherrimus* from the Upper Triassic Fleming Fiord Formation of East Greenland and a reassessment of the contribution of head lifting to feeding in temnospondyls. Journal of Vertebrate Paleontology 26: 223-247.

Kastschenko, N., 1881. Über die Genese und Architektur der Batrachierknochen. Archiv für mikroskopische Anatomie 19: 3-52.

Kin, A., Błażejowski, B. & Binkowski, M.M., 2012. The 'Polish Solnhofen': a long awaited alternative? Geology Today 28: 91-94.

Klein, N., 2010. Long bone histology of Sauropterygia from the Lower Muschelkalk of the Germanic Basin provides unexpected implications for phylogeny. PLoS ONE 5(7), e11613. doi:10.1371/journal.pone.0011613.

Klein, N. & Sander, M., 2008. Ontogenetic stages in the long bone histology of sauropod dinosaurs. Paleobiology 34: 247-263.

Köhler, M., Marín-Moratalla, N., Jordana, X. & Aanes, R., 2012. Seasonal bone growth and physiology in endotherms shed light on dinosaur physiology. Nature 487: 358-361.

Konietzko-Meier, D. & Klein, N., 2013. Unique growth pattern of *Metoposaurus diagnosticus krasiejowensis* (Amphibia, Temnospondyli) from the Upper Triassic of Krasiejów, Poland. Palaeogeography, Palaeoclimatology, Palaeoecology 370: 145-157.

Konzhukova, E.D., 1955. The Permian and Triassic labyrinthodonts of the Volga Basin and Cis-Urals. Trudy Paleozoologicheskogo Instituta, Akademia Nauk SSSR 49: 5-88 (in Russian).

Kuhn, J.L., Goldstein, S.A., Feldkamp, L.A., Goulet, R.W. & Jesion, G., 1990. Evaluation of a micro-computed tomography system to study trabecular bone-structure. Journal of Orthopaedic Research 8: 833-842.

Molnar, J.L., Pierce, S.E., Clack, J.A. & Hutchinson, J.R., 2012. Idealized landmark-based geometric reconstructions of poorly preserved fossil material: a case study of an early tetrapod vertebra. Palaeontologia Electronica 15: 1-18.

Moreno, K., Carrano, M.T. & Snyder, R., 2007. Morphological changes in pedal phalanges through ornithopod dinosaur evolution: a biomechanical approach. Journal of Morphology 268: 50-63.

Nilsson, T., 1934. Vorläufige Mitteilung über einen Stegocephalenfund aus dem Rhät Schonens. Geologiska Föreningens i Stockholm Förhandlingar 56: 428-442.

Nilsson, T., 1937. Ein Plagiosauride aus dem Rhät Schonens. Beiträge zur Kenntnis der Organisation der Stegocephalengruppe Brachyopoidei. Meddelanden från Lunds Geologisk-Mineralogiska Institution 72: 1-75.

Nilsson, T., 1946. A new find of *Gerrothorax rhaeticus* Nilsson, a plagiosaurid from the Rhaetic of Scania. Lunds Universitets Årsskrift, N.F. 42: 1-42.

Novikov, I.V. & Shishkin, M.A., 1992. New Middle Triassic labyrinthodonts from the Pechora Urals. Paleontological Journal 26: 92-102.

Ponce de León, M.S. & Zollikofer, C.P.E., 1999. New evidence from Le Moustier 1: computer-assisted reconstruction and morphometry of the skull. The Anatomical Record 254: 474-489.

Rozenblut, B. & Ogielska, M., 2005. Development and growth of long bones in European water frogs (Amphibia: Anura: Ranidae), with remarks on age determination. Journal of Morphology 265: 304-317.

Ruf, I., Luo, Z. & Martin, T., 2010. CT scanning analysis of the basicranium and the inner ear of *Haldanodon exspectatus* (Docodonta, Mammalia). Journal of Vertebrate Paleontology, Abstracts and Program 2010: 154A.

Sanchez, S., De Ploëg, G., Clément, G. & Ahlberg, P.E., 2010a. A new tool for determining degrees of mineralization in fossil amphibian skeletons: the example of the Late Palaeozoic branchiosaurid *Apateon* from the Autun Basin, France. Comptes Rendus Palevol 9: 311-317.

Sanchez, S., Germain, D., De Ricqlès, A., Abourachid, A., Goussard, F. & Tafforeau, P., 2010b. Limb-bone histology of temnospondyls: implications for understanding the diversification of palaeoecologies and patterns of locomotion of Permo-Triassic tetrapods. Journal of Evolutionary Biology 23: 2076-2090.

Sander, P.M., 2000. Long bone histology of the Tendaguru sauropods: implications for growth and biology. Paleobiology 26: 466-488.

Sander, P.M., Klein, N., Stein, K. & Wings, O., 2011. Sauropod bone histology and its implications for sauropod biology. *In:* Klein, N., Remes, K., Gee, C.T. & Sander, P.M. (eds.): Biology of the sauropod dinosaurs: understanding the life of giants. Indiana University Press (Bloomington): 276-302.

Sander, P.M., Klein, N., Buffetaut, E., Cuny, G., Suteethorn, V. & LeLoeuff, J., 2004. Adaptive radiation in sauropod dinosaurs: bone histology indicates rapid evolution of giant body size through acceleration. Organisms, Diversity & Evolution 4: 165-173.

Schoch, R.R., 2003. Early larval ontogeny of the Permo-Carboniferous temnospondyl *Sclerocephalus*. Palaeontology 46: 1055-1072.

Schoch, R.R. & Witzmann, F., 2012. Cranial morphology of the plagiosaurid *Gerrothorax pulcherrimus* as an extreme example of evolutionary stasis. Lethaia 45: 371-385.

Schwarz, C., Ruf, I. & Martin, T., 2010. Micro-CT analysis of the ear region in *Heteroxerus costatus* (Rodentia, Mammalia). Journal of Vertebrate Paleontology, Abstracts and Program 2010: 160A.

Sellers, W.I., Manning, P.L., Lyson, T., Stevens, K. & Margetts, L., 2009. Virtual palaeontology: gait reconstruction of extinct vertebrates using high performance computing. Palaeontologica Electronica 12(3): 13A. www.palaeo-electronica.org/2009_3/180/.

Shishkin, M.A., 1967. Plagiosaurs from the Triassic of the USSR. Paleontologicheskii Zhurnal 1967(1): 86-92 (in Russian).

Shishkin, M.A., 1986. New data on plagiosaurs from the Triassic of the USSR. Byulletin' Moskovskogo Obshchestva Ispytatelej Prirody, Otdel Geologicheskij 61: 97-102 (in Russian).

Shishkin, M.A., 1987. Evolution of ancient amphibians. Trudy Paleontologicheskogo Instituta, Akademiia Nauk SSSR 225: 3-12 (in Russian).

Starck, J.M. & Chinsamy, A., 2002. Bone microstructure and developmental plasticity in birds and other dinosaurs. Journal of Morphology 254: 232-246.

Stein, K. & Sander, M., 2009. Histological core drilling: a less destructive method for studying bone histology. *In:* Brown, M.A., Kane, J.F. & Parker, W.G. (eds): Methods in fossil preparation. Proceedings of the First Annual Fossil Preparation and Collections Symposium: 69-80.

Steyer, J.S., Laurin, M., Castanet, J. & De Ricqlès, A., 2004. First histological and skeletochronological data on temnospondyl growth: palaeoecological and palaeoclimatological implications. Palaeogeography, Palaeoclimatology, Palaeoecology 206: 193-201.

Suteethorn, V., Janvier, P. & Morales, M., 1988. Evidence for a plagiosauroid amphibian in the Upper Triassic Huai Hin Lat Formation of Thailand. Journal of Southeast Asian Earth Science 2: 185-187.

Von Huene, F., 1922. Beiträge zur Kenntnis der Organisation einiger Stegocephalen der schwäbischen Trias. Acta Zoologica 3: 395-459.

Warren, A.A., 1995. *Plagiosternum granulosum* E. Fraas: a plagiosaurid temnospondyl from the Middle Triassic of Crailsheim, Germany. Stuttgarter Beiträge zur Naturkunde B229: 1-8.

Witzmann, F., 2005. Hyobranchial and postcranial ontogeny of the temnospondyl *Onchiodon labyrinthicus* (Geinitz, 1861) from Niederhäslich (Döhlen Basin, Autunian, Saxony). Paläontologische Zeitschrift 79: 479-492.

Witzmann, F., 2006. Cranial anatomy and ontogeny of the Permo-Carboniferous temnospondyl *Archegosaurus decheni* from the Saar-Nahe Basin, Germany. Transactions of the Royal Society of Edinburgh, Earth Sciences 96:131-162.

Witzmann, F., 2009. Comparative histology of sculptured dermal bones in basal tetrapods, and the implications for the soft tissue dermis. Palaeodiversity 2: 233-270.

Witzmann, F., 2011. Morphological and histological changes of dermal scales during the fish-to-tetrapod transition. Acta Zoologica (Stockholm) 92: 281-302.

Witzmann, F. & Schoch, R.R., 2006. The postcranium of *Archegosaurus decheni*, and a phylogenetic analysis of temnospondyl postcrania. Palaeontology 49: 1211-1235.

Witzmann, F. & Soler-Gijón, R., 2010. The bone histology of osteoderms in temnospondyl amphibians and in the chroniosuchian, *Bystrowiella*. Acta Zoologica (Stockholm) 91: 96-114.

Witzmann, F., Scholz, H. & Ruta, M., 2009.The skull ontogeny of temnospondyls: a geometric morphometrics approach. Alcheringa 33: 237-255.